Check for updates

Enhancing data collection for palaeoenvironmental approaches in anthracology: X-ray microCT and ecological anatomy

Cristina Marilin Calo[1,2]* and Bernarda Marconetto[2]

[1]Museu de Arqueologia e Etnologia, Universidade de São Paulo, São Paulo, Brazil, [2]Instituto de Antropología de Córdoba, Universidad Nacional de Córdoba-Conicet, Córdoba, Argentina

X-ray microtomography has emerged as a valuable technique in archaeology for over a decade, aiding in the recording, preservation, and analysis of artifacts. While its application to archaeobotanical remains is well-documented, its use to study archaeological wood charcoal remains limited to preliminary research. This work explores microtomography suitability for anthracological studies based on a paleoenvironmental perspective. Ten Amazonian wood charcoal samples were studied using experimental charring, X-ray microCT and image data processing and analysis. 2D and 3D measures of anatomical attributes sensitive to environmental conditions, integrated as vulnerability index and mineral bodies abundance, were performed and compared. Results indicate that 3D imaging yields comparable insights to 2D analysis while being more efficient. The study highlights the benefits of volumetric data in vulnerability index calculations and crystal quantification, providing greater accuracy than traditional 2D methods. While further validation is needed, microtomography shows promise in enhancing the speed and reliability of anthracological studies.

KEYWORDS

X-ray microtomography, 3D imaging, archaeobotany, experimental wood charcoal, paleoenvironmental reconstruction, plant vulnerability index, calcium oxalate crystals, Amazonian wood

Introduction

X-ray microtomography was brought among the methodological spectrum of archaeology over a decade ago. Since then it has been implemented in the recording and documentation of objects and collections, characterization of archaeological artifacts, materials and manufacturing procedures, as well as the analysis of site-formation processes and taphonomy.

A considerable number of scientific articles has been dedicated to explore the suitability of microtomography for archaeobotanical studies (Ngan-Tillard et al., 2015; Murphy and Fuller, 2017; Zong et al., 2017; Barron and Denham, 2018; Calo et al., 2019, 2020; Pritchard et al., 2019; Barron et al., 2022). Microtomography has been used to specifically analyze wood and bark archaeological objects focusing on taphonomy (Haneca et al., 2012), conservation (Puhar et al., 2022), chronology (Stelzner and Million, 2015) and taxonomic

identification (Dreossi et al., 2010; Mizuno et al., 2010; Whitau et al., 2016; Zhao et al., 2018; Stelzner I. et al., 2023; Stelzner J. et al., 2023).

MicroCT-based approaches to wood charcoal are sparse and limited to experimental analysis and preliminary results. These are centered in testing their suitability regarding the analysis of morphologic diagnostic attributes (Hubau et al., 2013; Calo and Marconetto, 2024) or the presence of substances that might disturb radiocarbon dating results (Bird et al., 2008). Applications in anthracological research on charcoal assemblages from archaeological contexts, either focused on past environments characterization or the management of woody resources, do not yet have published works.

This gap is rather a consequence of some issues concerning its application for anthracological studies than the perceived novelty of the X-ray microtomography imaging. A previous paper by Calo and Marconetto (2024) suggests that microtomography offers only limited usefulness for anatomic descriptions aimed toward the identification of numerous charcoal fragments. This is mainly due to the compromise between time and cost involved in X-ray imaging for huge sets of samples as well as the lower degree of detail achieved in visualizing diagnostic features when compared to light microscopy.

However, the authors indicate some benefits of microtomography that partly equalize these constraints and may contribute to alternative perspectives in studying archaeological wood charcoal. Two of them are of special interest in this work. First, its suitability to provide qualitative and quantitative morphologic data in an automated, fast and efficient way. Second, its ability to reduce observational and statistical biases, derived from the three-dimensional character of the microCT image data. Descriptions and measurements on the anatomic attributes of three-dimensional objects do not rely on a cutting surface (2D) but on sequences of numerous and multidirectional layers that can be virtually obtained on their 3D models. This process considerably increases the amount of information available to describe several anatomic attributes (Calo and Marconetto, 2024).

Unlike qualitative and presence/absence information, quantitative morphologic data usually receive limited attention for taxonomic identification of anthracological material. This limitation is mainly explained because charring notably and variably alters the diagnostic dimensional attributes of wood (e.g., Marconetto, 2008). Likewise, populations of the same plant taxon growing under different environmental conditions may have changes in size, number and distribution of certain anatomic attributes (Carlquist, 1977, 1988). Carbonization and environmental growth conditions both can contribute to blur some of the quantitative characteristics used to distinguish different taxa and hinder their identification.

Notwithstanding, these kinds of issues turn in analytical pathways when observed from a diverse perspective. If anatomical changes due to environmental differences can be traced from quantifiable besides qualitative attributes in wood (and charcoal) then these might provide useful data to anthracogically describe paleoenvironments (Marconetto, 2010). Ecological Anatomy provides a theoretical and methodological basis for anthracological studies oriented to interpret high resolution environmental differences in geographical and chronological terms, based on quantitative and qualitative information on the structure of the xylem (Carlquist, 1988). According to it, for instance, the degree of vulnerability of a tree population to changes in water availability can be quantified or the characteristics of the soil where trees grow can be assessed.

The vulnerability index, determined by Carlquist (1977), allows to analyze the correlation between xylem anatomy and habitat type, assessing quantitative attributes of the woody tissue. The formula contemplates two variables: the size of the vessels, relatable to the efficiency of conduction, and the number of vessels as indicative of the conduction safety. Lower values of this index along samples of the same taxon indicate drier environments and higher values indicate more humid ones (Laskowski, 2000). To date, the determination of the vulnerability index has been based on two-dimensional measurements on elements of the plant conduction system.

Vulnerability index as a proxy in environmental and paleoenvironmental studies reports on anatomical variations through a single species. The inter-taxa variability is also linked

TABLE 1 X-ray microCT experimental parameters in image acquisition (SDD, Source-Detector Distance; SOD, Source-Object Distance).

| Sample	Energy (KeV)	Current (mA)	SDD (mm)	SOD (mm)	Sector (°)	Angle (°)	Projections (n)	Pixel size (μm)
Anacardium giganteum	80	200	817.22	23.23	360	0.18	2,000	5.68
Brosimum paraense	80	200	817.22	22.57	360	0.18	2,000	5.52
Calycophyllum spruceanum	70	170	817.22	20.44	360	0.18	2,000	5.00
Cedrela odorata	70	200	817.22	22.18	360	0.18	2,000	5.43
Copaifera sp	90	100	817.22	24.54	360	0.18	2,000	6.00
Diplotropis martiusii	70	170	817.22	20.44	360	0.18	2,000	5.00
Hura crepitans	70	200	817.22	21.75	360	0.18	2,000	5.32
Licania sp	80	200	817.22	23.40	360	0.18	2,000	5.72
Micropholis sp	70	170	817.22	22.50	360	0.18	2,000	5.51
Ocotea cymbarum	70	200	817.22	22.07	360	0.18	2,000	5.40
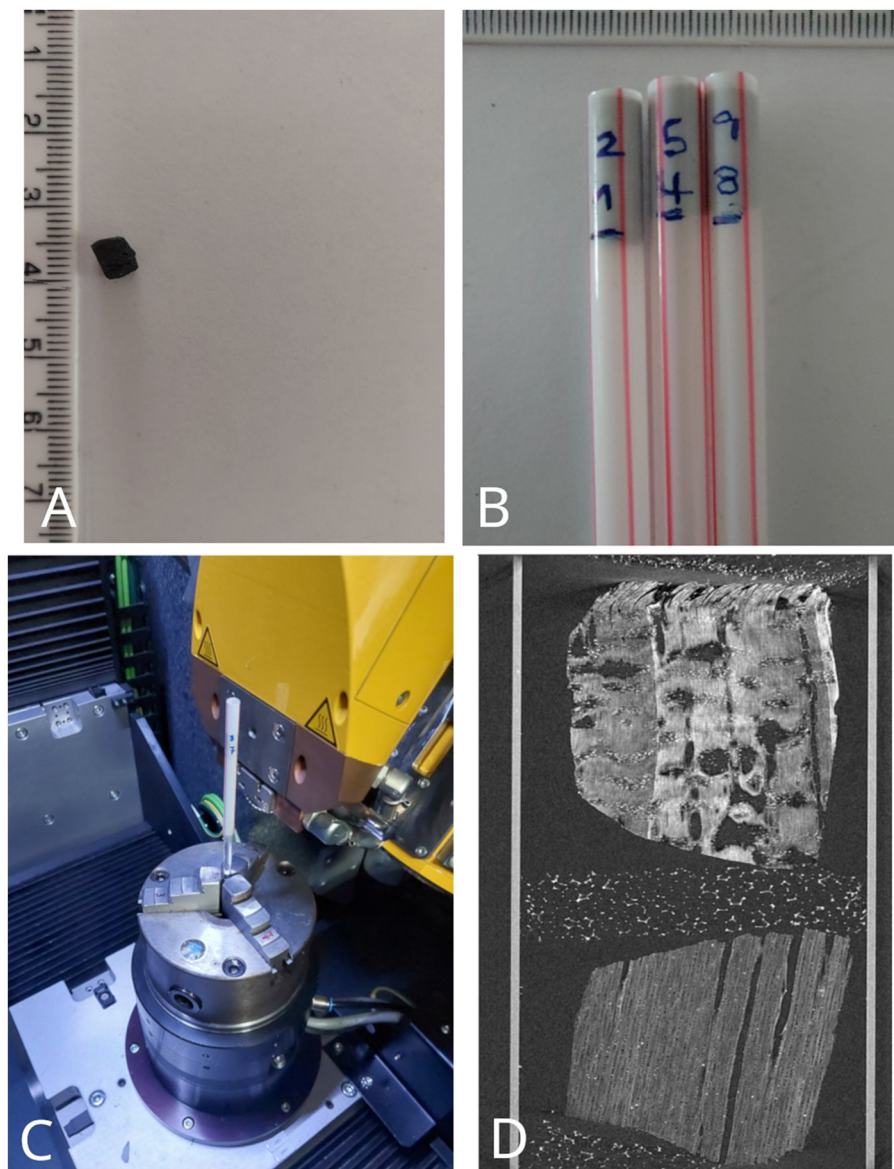
FIGURE 1
Sample preparation and assembly for X-ray microCT image acquisition: **(A)** a carved 4 mm side cube of wood charcoal; **(B)** Polypropylene tubes each containing a pair of charcoal samples; **(C)** Polypropylene tube assembly in the Phoenix microCT system holder; **(D)** Longitudinal section of a microtomography image showing the setup of a pair of charcoals (Extracted from Calo and Marconetto, 2024).
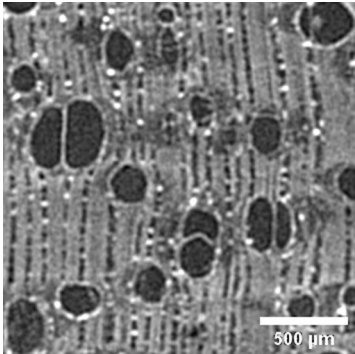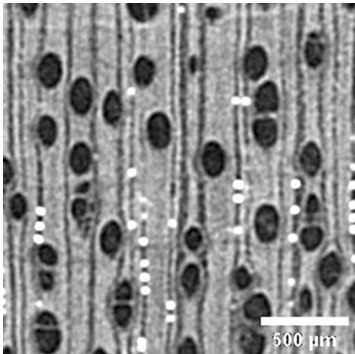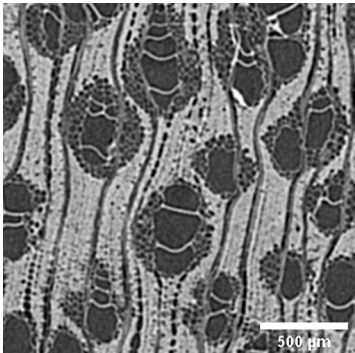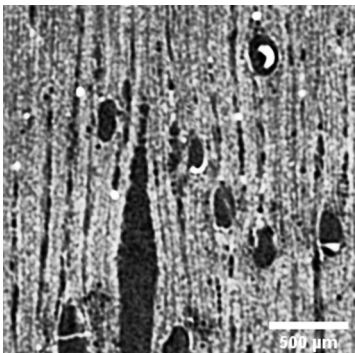
to genetic factors as suggested by the assemblage of sample woods used to tunning the application of the index in León Hernández (2014) and León Hernández (2020). Variations in wood anatomical characters has been mainly measured at synchronous scale based on species growing in different places around the globe (Baas and Carlquist, 1985). Diachronic scale application of the vulnerability index is present in paleobotanical studies (Poole, 1994; Brea et al., 2005) and archaeological charcoal analysis (Marconetto, 2009, 2010).

The potential of mineral bodies variability in wood as an environmental proxy has been less examined and discussed than the xylem anatomy. However, it has been suggested that the abundance of crystals in wood relates to the characteristics of the soil where trees grow. Plants absorb several elements such as Fe, K, N and huge amounts of Ca from soils and stock them in tissues and organs (Franceschi and Horner, 1980; Espinoza de Pernía, 1987). Likewise, high Ca concentration in soil leads to the formation of crystalline bodies, generally oxalates, in order to maintain the plant ion balance (Rasmussen and Smith, 1961; Espinoza de Pernía, 1987).
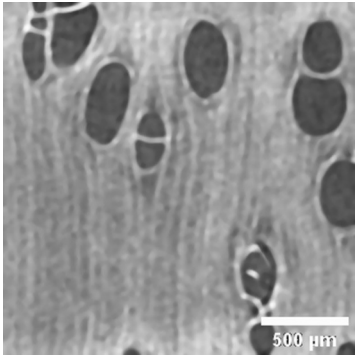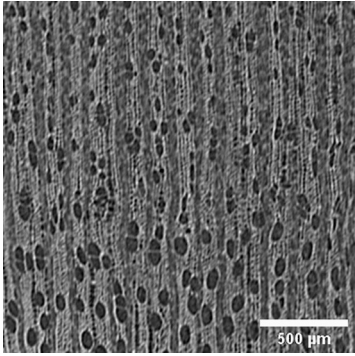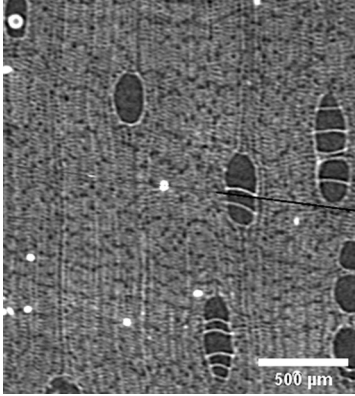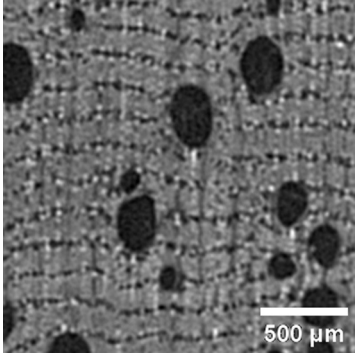
León Hernández and Espinosa de Pernía (1997) pointed that habitat and specially soil characteristics, in addition to the genetic component, might impact in crystal types and amounts present in *Cordia thaisiana* specimens growing in different woodland preserved areas. In turn, Ca concentration in soils depends on the volume of water carrying Ca. In rich-water basins Ca concentration is lower and this reflects in the amounts of Ca crystals present in plants wood and *viceversa*. Lower water temperature also interferes in reducing Ca transportation and cold waters tend to contain less Ca than the warmer ones.

TABLE 2 Anatomic characterization of the transversal section of the samples.

Sample / Specie	Anatomic description	Microtomographic slice
Anacardium giganteum ANACARDIACEAE	Growth ring boundaries: indistinct/Porosity: diffuse/Vessel groupings: solitary, occasionally 2–3 elements/ Axial parenchyma: aliform/Crystals observed (Cfr. Ugarte Oliva, 2009).	
Brosimum paraense sin. *B. rubescens* MORACEA	Growth ring boundaries: indistinct or absent/Porosity: wood diffuse-porous; Vessel groupings: solitary mostly and 2–4 elements groups/Axial parenchyma: paratracheal aliform thin./Crystals observed in rays (Cfr. Richter and Dallwitz, 2000).	
Calycophyllum spruceanum RUBIACEAE	Growth ring boundaries: indistinct/Porosity: semi-ring-porous/Vessel groupings: radial pattern, solitary and 2 elements/ Axial parenchyma: absent or rare (Cfr. Baldin et al., 2016; Gálvez et al., 2020).	
Cedrela odorata MELIACEAE	Growth ring boundaries: distinct by porous and bands of marginal parenchyma/Porosity: semi ring/Vessel groupings: solitary and 2–3 elements/ Axial parenchyma: marginal, vasicentric paratracheal and diffuse apotracheal (Cfr. León Hernández, 2020).	
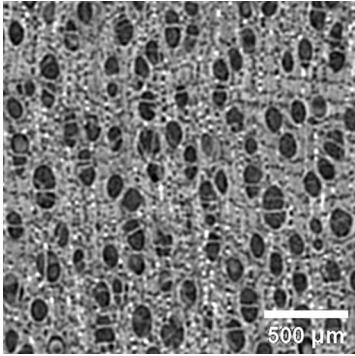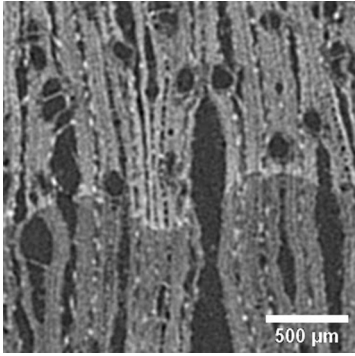
(Continued)

TABLE 2 (Continued)

Sample / Specie	Anatomic description	Microtomographic slice
Copaifera sp FABACEAE	Growth ring boundaries: indistinct/Porosity: semi-ring porous/Vessel groupings: solitary, radial series 2–4, scant clusters/ Axial parenchyma: apotracheal scant.	
Diplotropis martiusii sin. *Diplotropis purpurea* FABACEAE	Growth ring boundaries: indistinct/Porosity: diffuse /Vessel groupings: solitary and multiple radials 2–4/ Axial parenchyma: paratracheal aliform (Cfr. León Hernández, 2020).	
Hura crepitans EUPHORBIACEAE	Growth ring boundaries: indistinct/Porosity: diffuse/Vessel groupings: solitary and multiple radials 2–3/Axial parenchyma: apotracheal diffuse and in aggregates; scant paratracheal (Cfr. León Hernández and Chavarri, 2006).	
Licania sp CHRYSOBALANACEAE	Growth ring boundaries: indistinct/Porosity: diffuse/Vessel groupings: solitary /Axial parenchyma: apotracheal in narrow bands and paratracheal scant/Crystals observed in rays.	

(Continued)

TABLE 2 (Continued)

Sample / Specie	Anatomic description	Microtomographic slice
Micropholis sp SAPOTACEAE	Growth ring boundaries: indistinct/Porosity: diffuse/Vessel groupings: radial pattern, 2–3 elements / Axial parenchyma: apotracheal in narrow bands.	500 μm
Ocotea cymbarum LAURACEAE	Growth ring boundaries: distinct by differences in fibers/Porosity: diffuse/Vessel groupings: solitary, radial pattern 2–4, occasionally clusters/ Axial parenchyma: paratracheal scant, thin, aliform occasionally confluent (Cfr. León Hernández, 2014).	500 μm

Scale bar: 500 μm.

The approach of Ecological Anatomy would enhance anthracological results for past environments research based on the determination of plant taxa association from charcoal assemblages and would circle the concomitant question about the effects of past human selection of woods in archaeological contexts (i.e., Chabal, 1997; Asouti and Austin, 2005; Marconetto, 2008). Differently to taxa-identification oriented studies, the ecological wood anatomy is focused on the characterization of specific anatomical features and relies on inter-comparable sample sets with predefined size and taxa composition.

However, reliable results mainly depend on the extraction of substantial sums of quantitative and qualitative data from large amounts of specific anatomic structures on a defined number of sampled charcoals. A considerable investment in processing time must be taken in account to the extent that low levels of automation are used for analysis procedures. In line with the above, this work proposes and examines X-ray microtomography imaging as an analytical method that can significantly streamline the process to obtain ecological anatomy information from wood charcoal fragments, optimizing time-saving analysis but also data accuracy.

Methodology

This work tracks X-ray microtomography and 3D analysis performance for anatomic characterization of wood charcoal focusing on quantitative data and ecological anatomy variables. It compares results in the vulnerability index and presence/quantity of mineralizations/crystals along several species of trees based on 2D and 3D information. Ten fragments of experimental charred wood obtained from the anthracological reference collection of the Museum of Archaeology and Ethnology of the University of São Paulo (MAE-USP) were studied (Table 1).

The whole controlled experimental charring procedures on the studied woods were performed at the MAE-USP laboratories. Wood fragments were deshumidified in a FANEM model 515 stove for a period of 5 h at 40–50°C to prevent damages in anatomic structures by abrupt steam releases which could occur during the later charring process. Once the samples were mostly dry, they were individually wrapped in aluminum foil, arranged in metal trays and introduced into a muffle model FDG 3P-S of EDG Equipamentos. The carbonization parameters were normalized over a range of temperature increase starting at room temperature up to a maximum of 400°C. The rate of temperature increase was set at 2°C per min and once the maximum value was reached, it was maintained over a period of 40 min.

A cubic fragment of 4 mm side was obtained from each experimental charred sample with a scalpel. These prepared cubic charcoal sample were scanned in pairs using a Phoenix X-ray microCT system, model v|tome|x *m* (General Electric Company), at the Laboratory of Computerized Microtomography and 3D Image Processing of the Zoology Museum of USP. Polypropylene tubes and floral foam were used for mounting the samples on the object-holder of the microCT device, as shown in Figure 1. Experimental acquisition parameters were kept within a close range of values over the whole set of studied samples (Table 1),

TABLE 3 Results from 3D image data.

Sample	Total Volume (mm^3)	Volume of tissues (mm^3)	Volume of pores (mm^3)	Number of pores (n)	Vulnerability Index in 3D	Number of mineral bodies (n/mm^3)
Anacardium giganteum	8.04	6.92	1.11	24	4.63	1,918.63
Brosimum paraense	8.05	7.01	1.04	40	2.61	285
Calycophyllum spruceanum	8.03	6.77	1.26	50	2.52	0
Cedrela odorata	8.06	7.67	0.39	10	3.89	22.13
Copaifera sp	8.07	6.92	1.15	15	7.68	0
Diplotropis martiusii	8.03	7.49	0.54	203	0.26	0
Hura crepitans	8.62	7.97	0.65	18	3.61	77.5
Licania sp	8.05	7.32	0.73	15	4.89	4,630.88
Micropholis sp	8.06	6.82	1.24	127	0.98	5,938.5
Ocotea cymbarum	8.04	7.82	0.23	17	1.33	2,120.63

TABLE 4 Results from 2D image data.

Sample	Total area (mm^2)	Area of tissues (mm^2)	Area of pores (mm^2)	Number of pores (n)	Vulnerability index in 2D	Number of mineral bodies (n/mm^2)
Anacardium giganteum	4.00	3.48	0.53	20	2.64	40.75
Brosimum paraense	4.02	3.49	0.53	42	1.26	8.25
Calycophyllum spruceanum	4.00	3.22	0.78	49	1.60	0
Cedrela odorata	4.01	3.78	0.24	10	2.37	8
Copaifera sp	4.02	3.45	0.57	13	4.40	0
Diplotropis martiusii	4.00	3.77	0.23	150	0.16	0
Hura crepitans	4.30	3.97	0.33	13	2.50	2.5
Licania sp.	4.02	3.66	0.36	15	2.41	76
Micropholis sp.	4.02	3.40	0.62	130	0.47	112
Ocotea cymbarum	4.01	3.85	0.16	16	1.00	39.75

minimizing acquisition bias for subsequent analysis and results. However, as image contrast level and resolution were prioritized, some variations were conceded to compensate for inherent wood density differences across the charcoal sample set. Likewise, the parameterization also accounted for unpredictable divergences resulting from the scalpel-sculpting and positioning of the charcoal cubes in the sample mounting array. The Phoenix datos|x software, provided by the microCT system manufacturer, was used to reconstruct the microtomography images.

MicroCT image processing and analysis was performed using the Fiji distribution of ImageJ software (Schindelin et al., 2012, 2015; Rueden et al., 2017). Because the scanned charcoal cubes had been scalpel-trimmed without matching the position of the

three anatomical planes for wood analysis their virtual models were re-sectioned to enhance the visualization of the transverse (TS), radial longitudinal (RLS) and tangential longitudinal (TLS) sections. This procedure entailed cropping the size of the image into 2-mm-sided virtual cubes (∼300–400 pixels side, depending on the scanned sample), where measurements and counting were effectively performed.

The Median 3D image filter was applied (x, y, z radius: 4.0 to 6.0) to each gray-scale charcoal image in order to minimize noise. Segmentation into wood tissues, mineral bodies and background pixels was obtained by binarization using mainly the auto-threshold Otsu method. Where appropriate, some 3D morphological filters for binarized images (Opening and Closing)
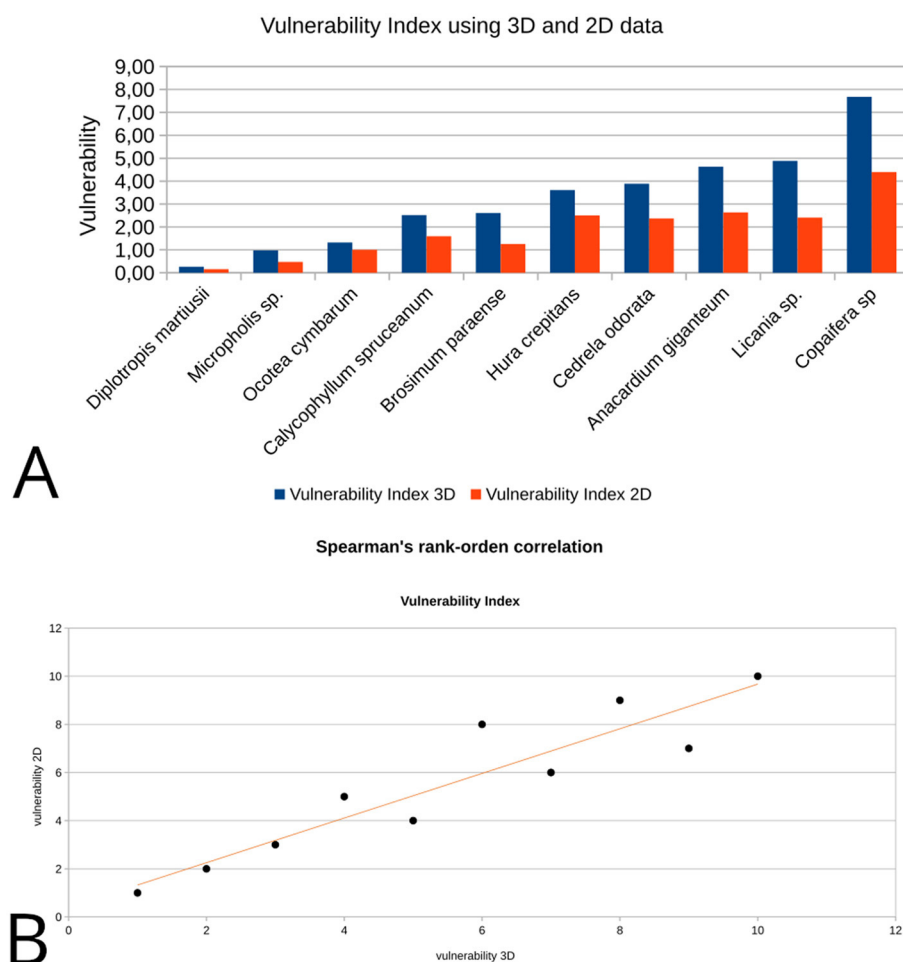
FIGURE 2
Vulnerability index estimation using 2D and 3D data: **(A)** the bar diagram comparatively displays absolute values of 2D and 3D vulnerability for each sample; **(B)** data scatter plot for the vulnerability Spearman's correlation coefficients from 2D to 3D data.

were applied using the Morpholib plugin in Fiji/ImageJ (Legland et al., 2016). Measures and counting for the assessment of the vulnerability index and number of mineral bodies in samples were performed on these binarized volumes (3D values) and single slices (2D values).

An adaptation to volumetric data of the vulnerability index formula in a previous article by Marconetto (2010) was applied in this study: $[V3D = (VP * VT)/P]$, where V = Vulnerability Index, VP = Pore Volume, VT = Total Volume and P = Pore Number. The pore values were obtained using the BoneJ2 plugin for Fiji/ImageJ (Domander et al., 2021) while the Object Counter tool was used for mineral bodies counting. On the other hand, 2D analysis employed the Analyze Particles tool both to measure pores and counting mineral bodies on randomly selected single slices.

Results

The Table 2 exhibits a concise description of the anatomical characters present in the TS for each charcoal sample based on their X-ray microCT image. Results of the 3D and 2D analysis

of anatomic characters for vulnerability index determination and quantification of mineral bodies are displayed in Tables 3, 4, respectively. The Figure 2A displays the vulnerability values for each species in increasing order showing a proportional ratio between 2D and 3D results beyond differences observed in absolute terms. A Spearman's rank-order correlation was run to determine the relationship between 2D and 3D results on vulnerability. There was a strong, positive correlation between these scores, which was statistically significant $[rs(8) = 0.927, p = 0.038$; Figure 2B]. Absolute differences must be associated with the divergences in geometry and measure units involved in the description of the 2D and 3D quantitative variables.

The number of mineral bodies per mm^2 and mm^3 also correlates the 3D and 2D values (Figures 3A, B). Likewise for vulnerability values, the Spearman's coefficient suggested a strong positive correlation statistically significant $[rs(8) = 0.975, p = 0.000001$; Figure 3C]. No mineral body was observed on the cross section in *Diplotropis martiusii*, *Calycophyllum spruceanum* and *Copaifera* sp and the same was observed in the whole volume. For the samples containing mineral bodies, total amounts between 30 and 450 units in a single slice (4 mm^2; see transversal slices included
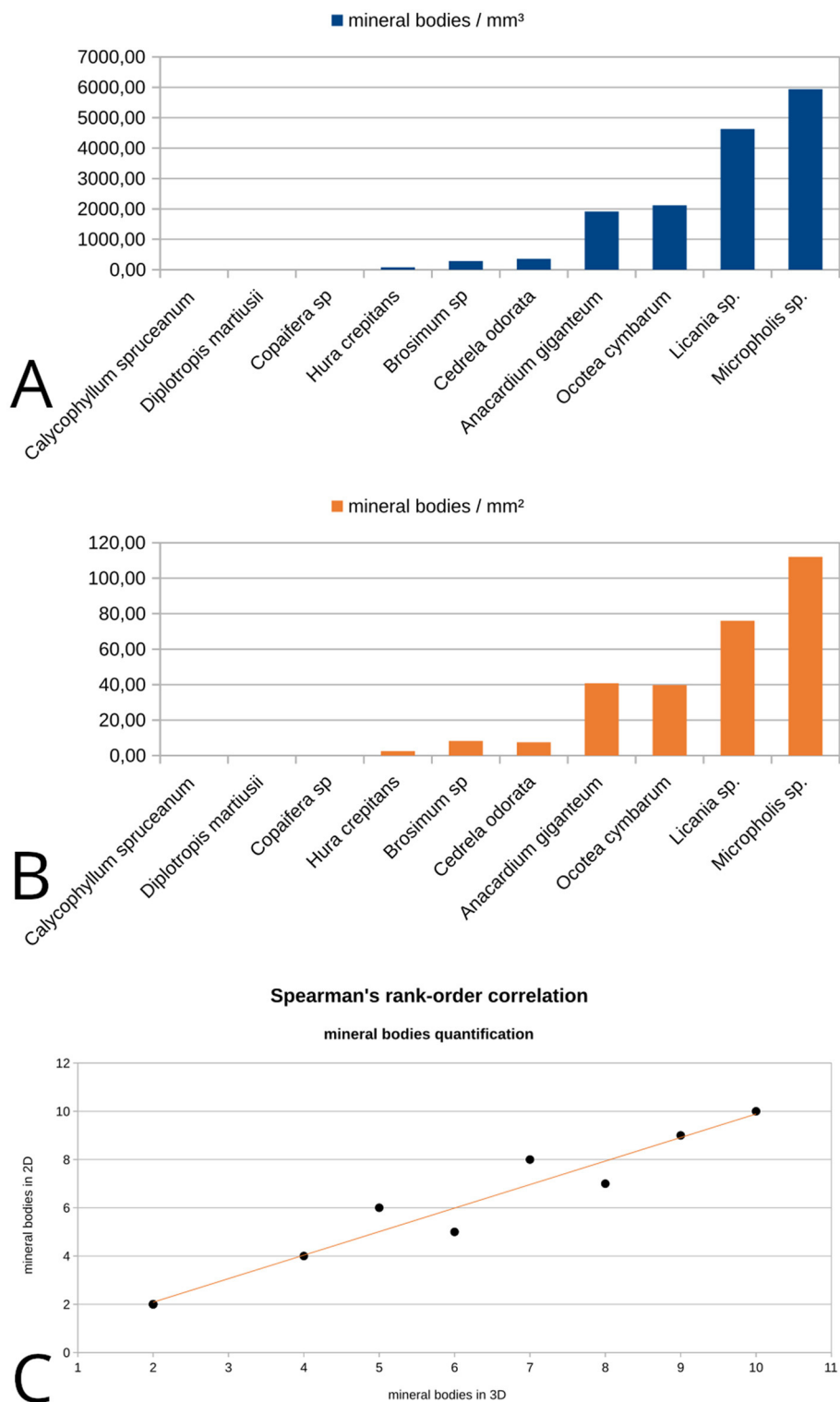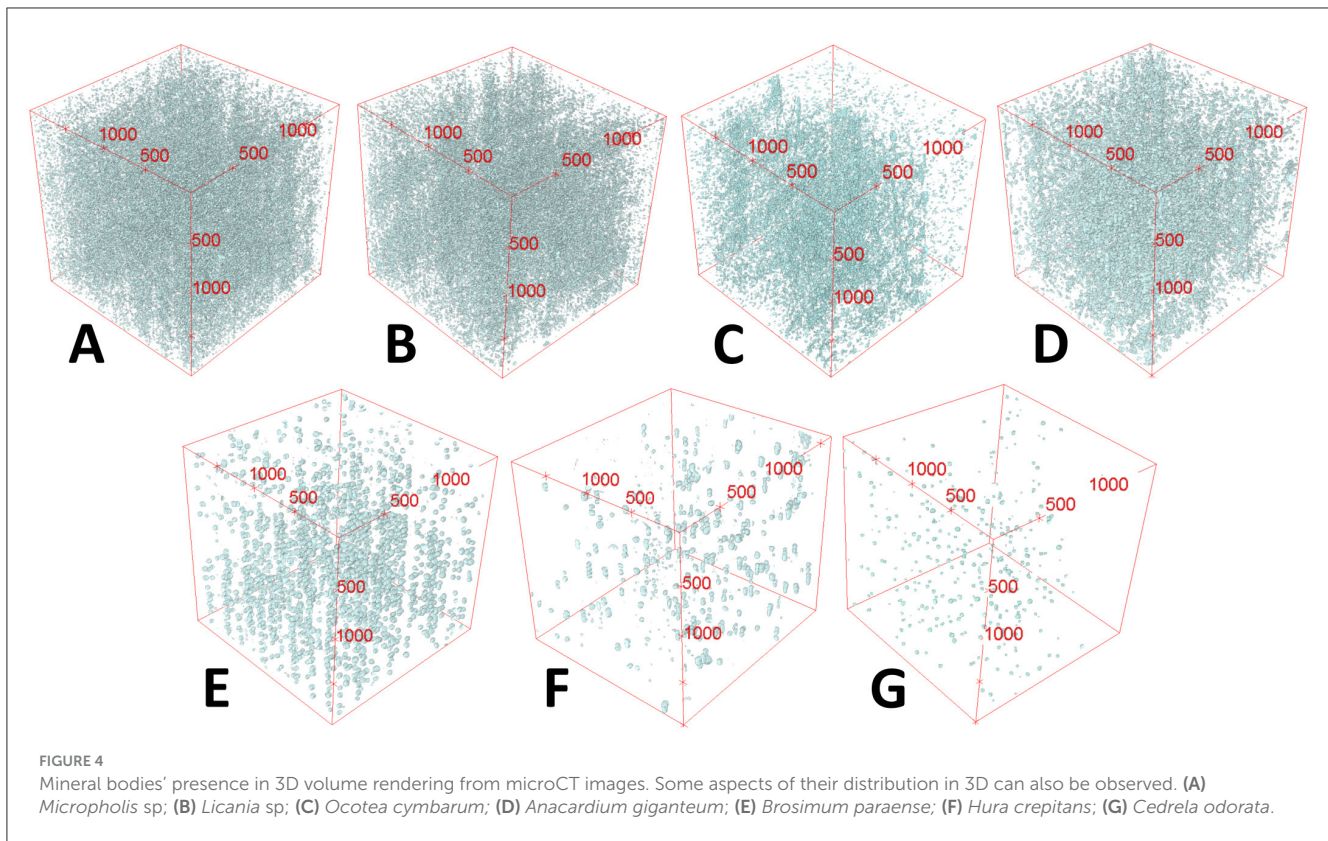
FIGURE 3
Mineral bodies quantification in 2D and 3D images: **(A)** number of mineral bodies per mm^3 in volume image for each sample; **(B)** number of mineral bodies per mm^2 in one single slice from each image/sample; **(C)** data scatter plot for mineral bodies presence Spearman's correlation coefficients from 2D to 3D data.

FIGURE 4
Mineral bodies' presence in 3D volume rendering from microCT images. Some aspects of their distribution in 3D can also be observed. **(A)** *Micropholis* sp; **(B)** *Licania* sp; **(C)** *Ocotea cymbarum*; **(D)** *Anacardium giganteum*; **(E)** *Brosimum paraense*; **(F)** *Hura crepitans*; **(G)** *Cedrela odorata*.

in Table 2) and between 70 and 6,000 units in volume (8 mm^3) were counted (Figure 4).

Conclusions

From Ecological Anatomy and Paleoenvironmental perspectives, these results present microtomography imaging analysis of anthracological material as a promising method to be used both for achieving accurate measurements based on volumetric data and providing information on very high frequency attributes in the studied objects. Quantitative characterization of a number of anatomical attributes can be accomplished in an automated, efficient and rather straightforward process using a suite of tools and functions available in an open-source/GPL image-processing software.

To better illustrate this point it might be useful to compare it with some aspects of the diachronic study on the variations of the vulnerability index in *Geoffroea decorticans,* carried out by Marconetto (2009) and Marconetto (2010). The anatomic analysis performed on 448 photomicrographs of the cross section of wood samples from 56 specimens entailed several months of non-automated work, complemented with the morphometry software Motic Images Plus 2.0. Regarding microtomography, once the image processing and segmentation have been standardized, retrieving the data pertinent to the vulnerability index computation takes place automatically through the application of specific algorithms yielding almost immediate results for each sample.

The reliability of volumetric anatomic data for vulnerability index assessment is suggested by the proportional correlation between these values and those obtained on two-dimensional data. The increase in the absolute values of the 3D vulnerability compared to those of the 2D vulnerability shown in Figure 2 could have its origin in the accumulation of information that each index entails. In this study, by contrasting the data from the entire sample with those from a single section of the sample, the information contained in the former is equivalent to what could be obtained on a set of 300 to 400 slices.

Another interesting contribution of microtomography as a method of analysis of wood charcoal is to provide an automated procedure to quantify the presence of mineral bodies and crystals as well as some morphological and compositional characteristics not addressed here (e.g., Calo et al., 2022). It might help to confirm the absence of mineral particles in specimens where they are very scarce. At the same time, it is able to quickly and accurately quantify their presence both within the entire sample volume and in a single cross-section.

This work proposed the usefulness of X-ray microtomography for anthracological research on past environments and other issues which can take advantage of its capabilities to generate precise volumetric data and efficiently quantify anatomical attributes. Indeed, automatized procedures allow the optimization of time dedicated to analysis when compared with non-automatized methods. Three-dimensional images not only enhance precision on porosity and vulnerability quantification on the xylem but also in detection and quantification of mineral bodies in charcoal

samples, opening new perspectives for paleoenvironmental and archaeological studies.

Data availability statement

The original contributions presented in the study are included in the article/supplementary material, further inquiries can be directed to the corresponding author.

Author contributions

CC: Conceptualization, Data curation, Formal analysis, Funding acquisition, Investigation, Methodology, Project administration, Resources, Software, Supervision, Validation, Visualization, Writing – original draft, Writing – review & editing. BM: Conceptualization, Formal analysis, Investigation, Methodology, Supervision, Validation, Writing – original draft, Writing – review & editing.

Funding

Acknowledgments

Conflict of interest

The authors declare that the research was conducted in the absence of any commercial or financial relationships that could be construed as a potential conflict of interest.

Generative AI statement

The author(s) declare that no Gen AI was used in the creation of this manuscript.

Publisher's note

All claims expressed in this article are solely those of the authors and do not necessarily represent those of their affiliated organizations, or those of the publisher, the editors and the reviewers. Any product that may be evaluated in this article, or claim that may be made by its manufacturer, is not guaranteed or endorsed by the publisher.

References

Asouti, E., and Austin, P. (2005). Reconstructing woodland vegetation and its exploitation by past societies, based on the analysis and interpretation of archaeological wood charcoal macro-remains. *Environ. Archaeol.* 10, 1–18. doi: 10.1179/env.2005.10.1.1

Baas, P., and Carlquist, S. (1985). A comparison of the ecological wood anatomy of the floras of southern California and Israel. *Iawa Bull.* 6, 349–353. doi: 10.1163/22941932-90000961

Baldin, T., Siegloch, A. M., and Marchiori, J. N. C. (2016). Compared anatomy of species of Calycophyllum DC (Rubiaceae). *Rev. Árvore* 40, 759–768. doi: 10.1590/0100-67622016000400020

Barron, A., and Denham, T. (2018). A microCT protocol for the visualisation and identification of domesticated plant remains within pottery sherds. *J. Archaeol. Sci. Rep.* 21, 350–358. doi: 10.1016/j.jasrep.2018.07.024

Barron, A., Pritchard, J., and Denham, T. (2022). Identifying archaeological parenchyma in three dimensions: diagnostic assessment of five important food plant species in the Indo-Pacific region. *Archaeol. Ocean.* 57, 189–213. doi: 10.1002/arco.5276

Bird, M. I., Ascough, P. L., Young, I. M., Wood, C. V., and Scott, A. C. (2008). X-ray microtomographic imaging of charcoal. *J. Archaeol. Sci.* 35, 2698–2706. doi: 10.1016/j.jas.2008.04.018

Brea, M.;, Matheos, S., Zamuner, A., and Gamuza, D. (2005). Análisis de los anillos de crecimiento del bosque fósil de Víctor Szlápelis, Terciario inferior del Chubut, Argentina. *Ameghiniana* 42, 407–418.

Calo, C. M., and Marconetto, B. (2024). Sobre el uso imágenes microtomográficas para estudios de carbón de madera arqueológico. *Rev. Mus. Antropol.* 17, 13–28. doi: 10.31048/py9r4w88

Calo, C. M., Rizzutto, M. A., Carmello-Guerreiro, S. M., Dias, C. S. B., Watling, J., Shock, M. P., et al. (2020). A correlation analysis of light microscopy and X-ray MicroCT imaging methods applied to archaeological plant remains' morphological attributes visualization. *Sci. Rep.* 10:15105. doi: 10.1038/s41598-020-71726-z

Calo, C. M., Rizzutto, M. A., Ferreira, C. G., Aguero, N. F., Pérez, C. A., Machado, R., et al. (2022). Some notes on dense structures present in archaeological plant remains: x-ray fluorescence computed tomography applications. *Minerals* 12:1130. doi: 10.3390/min12091130

Calo, C. M., Rizzutto, M. A., Watling, J., Furquim, L., Shock, M. P., Andrello, A. C., et al. (2019). Study of plant remains from a fluvial shellmound (Monte Castelo, RO, Brazil) using the X-ray MicroCT imaging technique. *J. Archaeol. Sci. Rep.* 26:101902. doi: 10.1016/j.jasrep.2019.101902

Carlquist, S. (1977). Ecological factors in wood evolution: a floristic approach. *Am. J. Bot.* 64, 887–896. doi: 10.1002/j.1537-2197.1977.tb11932.x

Carlquist, S. (1988). *Comparative Wood Anatomy: Systematic, Ecological, and Evolutionary Aspects of Dicotyledon Wood.* Berlin Heidelberg: Springer-Verlag (Springer Series in Wood Science). doi: 10.1007/978-3-662-21714-6

Chabal, L. (1997). "Chapitre 3. Une hypothèse. La représentativité paléoécologique des charbons de bois issus du bois de feu domestique," in *Forêts et sociétés en Languedoc (Néolithique final' Antiquité tardive) : L'anthracologie, méthode et paléoécologie.* Paris: Éditions de la Maison des sciences de l'homme (Documents d'archéologie française), 39–55. doi: 10.4000/books.editionsmsh.43440

Domander, R., Felder, A., and Doube, M. (2021). BoneJ2 - refactoring established research software [version 2; peer review: 3 approved]. *Wellcome Open Res.* 6:37. doi: 10.12688/wellcomeopenres.16619.2

Dreossi, D., Favretto, S., Fioravanti, M., Mancini, L., Rigon, L., Sodini, N., et al. (2010). "Synchrotron radiation micro-tomography: a non-invasive tool for the characterization of archaeological wood," in *Wood Science for Conservation of Cultural Heritage*, ed. L. Uzielli (Florence: Firenze University Press), 34–39.

Espinoza de Pernía, N. (1987). Cristales y sílice en maderas dicotiledóneas de latinoamérica. *Pittieria* 15, 13–65.

Franceschi, V. R., and Horner, H. T. (1980). Calcium oxalate crystals in plants. *Bot. Rev.* 46, 361–427. doi: 10.1007/BF02860532

Gálvez, G. I. E. C., Rocha, M. P., Klitzke, R. J., and Mora, H. E. G. (2020). Caracterización anatómica y variabilidad de los componentes de la

madera de *Calycophyllum spruceanum* (Benth). *Hook. Rev. Ciênc. Madeira* 11:2. doi: 10.12953/2177-6830/rcm.v11n2p93-106

Haneca, K., Deforce, K., Boone, M. N., Loo, D. V., Dierick, M., Acker, J. V., et al. (2012). X-ray sub-micron tomography as a tool for the study of archaeological wood preserved through the corrosion of metal objects. *Archaeometry* 54, 893–905. doi: 10.1111/j.1475-4754.2011.00640.x

Hubau, W., Bulcke, J. V. d., Kitin, P., Brabant, L., Acker, J. V., and Beeckman, H. (2013). Complementary imaging techniques for charcoal examination and identification. *IAWA J.* 34, 147–168. doi: 10.1163/22941932-000 00013

Laskowski, L. (2000). Características anatómicas de la hoja y el tallo del Semeruco (Mapighia Emarginata DC) cultivado en dos localidades del estado Lara. *Bioagro* 12, 33–40.

Legland, D., Arganda-Carreras, I., and Andrey, P. (2016). MorphoLibJ: integrated library and plugins for mathematical morphology with ImageJ. *Bioinformatics* 32, 3532–3534. doi: 10.1093/bioinformatics/btw413

León Hernández, W. J. (2014). Elementos xilemáticos de conducción en 69 especies leñosas de la reserva forestal caparo (Barinas, Venezuela). *Acta Botánica Venezuélica* 37, 91–121.

León Hernández, W. J. (2020). Anatomía de maderas de 130 especies de Venezuela. *Rev. Pittieria* 1–380.

León Hernández, W. J., and Chavarri R. B. N. (2006). Anatomía xilemática del tallo de 8 especies de la subfamilia Euphorbioideae (Euphorbiaceae) en Venezuela. *Rev. Fac. Agron* 106, 1–12.

León Hernández, W. J., and Espinosa de Pernía, N. (1997). Cristales en la madera de cordia thaisiana agostini. *Rev. For. Venez.* 41, 37–43.

Marconetto, M. B. (2008). *Recursos forestales y el proceso de diferenciación social en tiempos Prehispánicos en el Valle de Ambato, Catamarca, Argentina*. Oxford: J. and E. Hedges (BAR 1785). doi: 10.30861/9781407302164

Marconetto, M. B. (2009). Rasgos anatómicos asociados al estrés hídrico en carbón vegetal arqueológico, valle de ambato (catamarca), fines del primer milenio. *Darwiniana* 47, 247–259.

Marconetto, M. B. (2010). Paleoenvironment and anthracology: determination of variations in humidity based on anatomical characters in archaeological plant charcoal (Ambato Valley, Catamarca, Argentina). *J. Archaeol. Sci.* 37, 1186–1191. doi: 10.1016/j.jas.2009.12.016

Mizuno, S., Torizu, R., and Sugiyama, J. (2010). Wood identification of a wooden mask using synchrotron X-ray microtomography. *J. Archaeol. Sci.* 37, 2842–2845. doi: 10.1016/j.jas.2010.06.022

Murphy, C., and Fuller, D. Q. (2017). Seed coat thinning during horsegram (*Macrotyloma uniflorum*) domestication documented through synchrotron tomography of archaeological seeds. *Sci. Rep.* 7:5369. doi: 10.1038/s41598-017-0 5244-w

Ngan-Tillard, D., Dijkstra, J., Verwaal, W., Mulder, A., Huisman, H., and Müller, A. (2015). Under pressure: a laboratory investigation into the effects of mechanical loading on charred organic matter in archaeological sites. *Conserv. Manag. Archaeol. Sites* 17, 122–142. doi: 10.1080/13505033.2015.1124179

Poole, I. (1994). "Twig"-wood anatomical characters as palaeoecological indicators. *Rev. Palaeobot. Palynol.* 81, 33–52. doi: 10.1016/0034-6667(94)90125-2

Pritchard, J., Lewis, T., Beeching, L., and Denham, T. (2019). An assessment of microCT technology for the investigation of charred archaeological parenchyma from house sites at Kuk Swamp, Papua New Guinea. *Archaeol. Anthropol. Sci.* 11, 1927–1938. doi: 10.1007/s12520-018-0648-0

Puhar, E. G., Korat, L., Erič, M., Jaklič, A., and Solina, F. (2022). Microtomographic analysis of a palaeolithic wooden point from the ljubljanica river. *Sensors* 22:2369. doi: 10.3390/s22062369

Rasmussen, G. K., and Smith, P. F. (1961). Effects of calcium, potassium, and magnesium on oxalic, malic, and citric acid content of valencia orange leaf tissue. *Plant Physiol.* 36, 99–101. doi: 10.1104/pp.36.1.99

Richter, H. G., and Dallwitz, M. J. (2000). *Commercial Timbers: Descriptions, Illustrations, Identification, and Information Retrieval*. In English, French, German, and Spanish. Version: 4th May 2000. Available online at: http://biodiversity.uno.edu/delta/

Rueden, C. T., Schindelin, J., Hiner, M. C., DeZonia, B. E., Walter, A. E., Arena, E. T., et al. (2017). ImageJ2: imageJ for the next generation of scientific image data. *BMC Bioinform.* 18:529. doi: 10.1186/s12859-017-1934-z

Schindelin, J., Arganda-Carreras, I., Frise, E., Kaynig, V., Longair, M., Pietzsch, T., et al. (2012). Fiji: an open-source platform for biological-image analysis. *Nat. Methods* 9, 676–682. doi: 10.1038/nmeth.2019

Schindelin, J., Rueden, C. T., Hiner, M. C., and Eliceiri, K. W. (2015). The imageJ ecosystem: an open platform for biomedical image analysis. *Mol. Reprod. Dev.* 82, 518–529. doi: 10.1002/mrd.22489

Stelzner, I., Stelzner, J., Gwerder, D., Martinez-Garcia, J., and Schuetz, P. (2023). Imaging and assessment of the microstructure of conserved archaeological pine. *Forests* 14:211. doi: 10.3390/f14020211

Stelzner, J., and Million, S. (2015). X-ray computed tomography for the anatomical and dendrochronological analysis of archaeological wood. *J. Archaeol. Sci.* 55, 188–196. doi: 10.1016/j.jas.2014.12.015

Stelzner, J., Million, S., Stelzner, I., Nelle, O., and Banck-Burgess, J. (2023). Micro-computed tomography for the identification and characterization of archaeological lime bark. *Sci. Rep.* 13:6458. doi: 10.1038/s41598-023-33633-x

Ugarte Oliva, J. A. (2009). *Caracterización Anatómica de 9 Especies Forestales de la Concesión Industrial Maderera Zapote en Loreto* (Tesis de Grado). Universidad Nacional Agraria La Molina. Available online at: https://hdl.handle.net/20.500.12996/452

Whitau, R., Dilkes-Hall, I. E., Dotte-Sarout, E., Langley, M. C., Balme, J., and O'Connor, S. (2016). X-ray computed microtomography and the identification of wood taxa selected for archaeological artefact manufacture: rare examples from Australian contexts. *J. Archaeol. Sci. Rep.* 6, 536–546. doi: 10.1016/j.jasrep.2016.03.021

Zhao, G., Qiu, Z., Shen, J., Deng, Z., Liu, D., and Gong, J. (2018). Internal structural imaging of cultural wooden relics based on three-dimensional computed tomography. *BioResources* 13, 1548–1562. doi: 10.15376/biores.13.1.1548-1562

Zong, Y., Yao, S., Crawford, G. W., Fang, H., Lang, J., Fan, J., et al. (2017). Selection for oil content during soybean domestication revealed by x-ray tomography of ancient beans. *Sci. Rep.* 7:43595. doi: 10.1038/srep43595